THE ASTROPHYSICAL JOURNAL, 330:579–595, 1988 July 15

DISTANCES TO THE VIRGO AND URSA MAJOR CLUSTERS AND A DETERMINATION OF H_0

MICHAEL J. PIERCE[1] AND R. BRENT TULLY
Institute for Astronomy, University of Hawaii
Received 1987 October 23; accepted 1988 January 14

ABSTRACT

Multicolor CCD photometry of spiral galaxies within the Ursa Major and Virgo Clusters is presented and combined with accurate 21 cm H I line-width measurements in order to investigate the luminosity–line-width relations (Tully-Fisher [hereafter TF] relations) as a distance indicator. There is evidence for a slight morphological-type dependence of the TF relations, although the effect is present only at the 1–2 σ level. No difference in the slope of the TF relations is found between the two clusters, despite the considerable difference in densities and crossing times. A significant reduction in the dispersion of the TF relations is made possible from both accurate total magnitudes and accurate inclinations derived from ellipse fitting to galaxy isophotes. As a result, galaxies with inclinations as low as 30° can now be included in the sample. In the Ursa Major Cluster, the intrinsic dispersion in the TF relations is found to be only $\sim$0.25 mag. We show that the use of aperture magnitudes (e.g., H band data) results in an artificially large slope to the TF relations. The use of total magnitudes yields a slope of $\sim$8 at near-infrared wavelengths, as a result $L \propto V_{\max}^{3.2}$.

An absolute calibration of the TF relations was obtained by fitting to three nearby galaxies with reasonably accurate distances: M31, M33, and NGC 2403. These systems establish the distance to the Ursa Major Cluster to be 15.5 ± 1.2 Mpc and the mean distance to the Virgo Cluster to be 15.6 ± 1.5 Mpc, with slightly greater uncertainty due to the possible presence of superposed galaxies. A determination of the value of the Hubble Constant was made by assuming a Virgocentric flow of 300 km s^{-1} at the Local Group, yielding a derived value of $H_0 = 85 \pm 10$ km s^{-1} Mpc^{-1}.

Subject headings: cosmology — galaxies: clustering — galaxies: distances — galaxies: photometry — radio sources: 21 cm radiation

I. INTRODUCTION

The tight relationship between the luminosity of a spiral galaxy and its rotational velocity discovered by Tully and Fisher (1977) is generally recognized as the most promising intermediate-distance indicator in general use (Aaronson 1986). The luminosity–line-width relations (hereafter TF relations) have been employed by several groups working on the distance scale problem (e.g., Aaronson, Huchra, and Mould 1979; Bottinelli *et al.* 1983; Visvanathan 1983; Richter and Huchtmeier 1984; Sandage and Tammann 1984; Tully and Shaya 1984; Aaronson *et al.* 1986). Nevertheless, a controversy remains over the value of H_0 (see, e.g., de Vaucouleurs 1981; Sandage and Tammann 1982). With specific regard to the TF relations, there has been concern about morphological-type dependencies (Roberts 1978), uncertainty in the slope (Burstein *et al.* 1982), and Malmquist or related incompletion biases (Bottinelli *et al.* 1986; Sandage 1987; but see Giraud 1986). Moreover, there has been considerable uncertainty in the absolute calibration of the TF relations, for lack of reliable distances to nearby systems by alternative methods.

Recent developments in detector technology may result in an improvement of the status of the absolute calibration, with the application of Cepheid and RR Lyrae variables as primary distance indicators to a sufficient number of "local calibrators" (e.g., Madore 1985; Madore *et al.* 1985; Freedman 1985; Welch *et al.* 1986; Christian and Schommer 1987; Pritchet and van den Bergh 1987). It seems likely that in the next few years the distances to a number of nearby galaxies should be firmly established.

In this spirit of optimism we have undertaken a detailed study of the TF relations and their promise as a distance indicator using a large data base of high-quality CCD photometry and the latest 21 cm line widths. The TF relations are compared in such different environments as the Virgo Cluster core and the Ursa Major Cluster, with no significant differences revealed (§ III*b*). We address the question as to whether there is a morphological-type dependence to the TF relations (§ III*d*). We conclude that the intrinsic dispersion of the TF relations is quite small ($\sim$0.25 mag rms) and that with the proper extinction and inclination corrections the TF relations can provide distances with very high precision throughout a large range of galaxy environments. We find evidence for substructure in the Virgo Cluster and discuss some of the consequences (§ III*c*). We also discuss the variation in the slope of the TF relations with wavelength (§ III*d*). An adequate absolute calibration can be obtained from three galaxies with accurate distances: M31, M33, and NGC 2403 (§ IV*a*). We derive the distance to the Ursa Major and Virgo clusters and test the results for the effects of an incompletion bias (§ IV*c*). Given estimates of the Virgocentric velocity field, we derive the value of H_0 (§ V).

II. DATA AND ANALYSIS

a) Sample and Data Analysis

The sample of spiral galaxies discussed in this paper was selected from a photometric survey of $\sim$300 nearby galaxies (Pierce 1988). The subset discussed here consists of spiral galaxies within the Virgo Cluster (galaxies within 6° of M87 with

[1] This article is part of a dissertation to be submitted to the Graduate Division of the University of Hawaii in partial fulfillment of the requirements for the Ph.D. degree in Astronomy.

$V_0 < 3000$ km s^{-1}) and the Ursa Major Cluster (galaxies within 7°.5 of $\alpha = 11^h54^m$ $\delta = +49°30'$ with $700 < V_0 < 1210$ km s^{-1}). Here, systemic velocities V_0 were adjusted for motion of 300 km s^{-1} toward $l = 90°$, $b = 0°$. An estimate was made of the completeness of the two cluster samples as a function of apparent B magnitude by considering all non-E and non-S0 galaxies in the Center for Astrophysics (CfA) 14.5 mag survey (Huchra *et al.* 1983) within the domain of the two clusters and with velocities within the range prescribed above. Our CCD magnitudes were used if available, or Zwicky (1961–1963) magnitudes were corrected to $B_T^{b,i}$ magnitudes following the presciption given by Fisher and Tully (1981) with absorption corrections as specified by Tully and Fouqué (1985).

The completeness as a function of $B_T^{b,i}$ is shown in Figure 1. The top panel provides a histogram of the CfA 14.5 mag sample as a function of blue magnitude for the two clusters combined. It is seen that the sample becomes quite incomplete fainter than $B_T^{b,i} \approx 13.3$ mag, rather than as expected at 14.5 mag, principally due to a systematic error in Zwicky magnitudes at low surface brightness. The lower panel tracks our percentage completion of the CfA 14.5 mag sample. In calculating completion, galaxies have been excluded if (1) they are more face-on than 30°, (2) they have confused H I profiles, or (3) they have gross morphological peculiarities. The remaining galaxies are useful with respect to application of the TF relations if photometry and H I profiles with sufficient signal/noise are available. In the case of the Ursa Major Cluster, there is essentially completion of the CfA 14.5 mag sample, i.e., completion to $B_T^{b,i} \approx 13.3$ mag. In the case of the Virgo Cluster, unfavorable weather interrupted the photometry program, and there is only completion to $B_T^{b,i} \approx 12.0$ mag. In addition, randomly selected galaxies below the completion limit and as faint as $B_T^{b,i} \approx 15$ were included in both cluster samples.

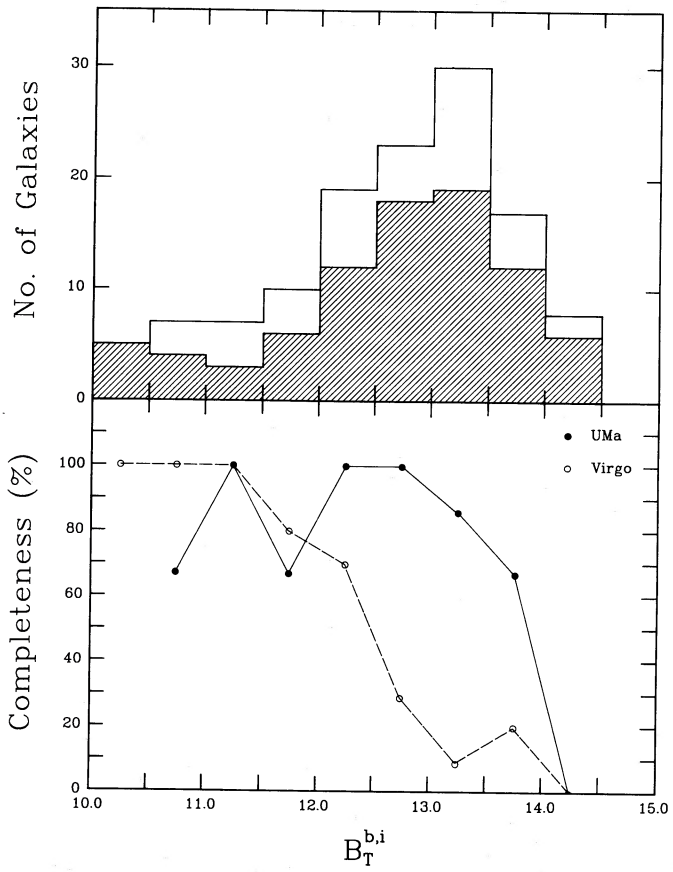

FIG. 1.—The sample completion as a function of apparent magnitude. *Top panel*: galaxies in the CfA 14.5 mag survey that satisfy the membership criteria of the Virgo (*shaded histogram*) and Ursa Major (*open histogram*) clusters, per magnitude interval. E and S0 types are excluded. Blue passband CCD magnitudes are used if available; otherwise, corrected Zwicky magnitudes are used. Adjustments are made for obscuration. *Bottom panel*: fractional completion of the present survey, per magnitude interval. A "complete" sample would include all non-E and non-S0 galaxies in the CfA 14.5 mag survey minus galaxies more face-on than 30°, or galaxies with confused H I profiles, or galaxies with gross morphological peculiarities. *Solid line* represents the Ursa Major Cluster, while *dashed line* represents the Virgo Cluster.

The sample germane to the TF relation will be discussed in the present paper. The photometric properties of a less restricted Virgo and Ursa Major sample will be discussed at a later date (Pierce 1988).

CCD imaging of the sample in the B, R_{KC}, and I_{KC} bandpass (KC denotes Kron-Cousins system; see Cousins 1976) was acquired over several seasons using the Galileo/Institute for Astronomy CCD camera. The camera employed a Texas Instruments thinned, backside-illuminated, 500 × 500 three-phase CCD (Hlivak *et al.* 1982). The detector was UV flooded during cool-down at the beginning of each run to improve the blue response as part of our standard procedure (Hlivak *et al.* 1984). The data were obtained in one of three observing configurations. In the first mode the CCD camera was placed behind a focal reducer at the Cassegrain focus of the 0.61 m University of Hawaii Planetary Patrol Telescope. The result is a field 13′ on a side with 1″.6 pixel^{-1} and an effective f ratio of f/3.2. Exposures were 10 minutes for the B bandpass and 5 minutes for the R and I bandpasses. Galaxies with diameters greater than 5′ were observed in this mode. The second mode involved the same configuration at the Cassegrain focus of the 2.2 m University of Hawaii Telescope. In this case the field is 5′.0 on a side with 0″.6 pixel^{-1} and an f ratio of f/2.3. The remainder of the cluster samples were acquired in this configuration with exposures of 5 minutes for the B bandpass and 150 s for R and I. The large apparent size of two nearby calibrating galaxies, M31 and M33, required a special configuration. These galaxies were imaged through a 1 inch telescope (105 mm Nikon lens) mounted on the 0.61 m telescope pointing up through the central baffle with the secondary removed. The field of view was 4°.1 with 29″.5 pixel^{-1}, and the lens was stopped down to f/4. The R band image of M31 is shown in Figure 2. Only B and R images were acquired for M31 and M33, as the lens coatings were highly reflective in the I bandpass. We plan to obtain I band photometry of these galaxies in the near future.

The images were bias subtracted and divided by normalized flat-field exposures of the dome (a large piece of white surfboard foam in the case of the 0.61 m data). Illumination was provided with a 3400 K tungsten lamp and a Wratten 80A filter in an attempt to simulate the broad-band colors of the night sky. Images of a region of blank sky were also obtained through each filter on each night. After the removal of stellar images these fields were fitted with two-dimensional third-order polynomials in order to remove any low-frequency background variations introduced by the flat-fielding process. This procedure resulted in blank-sky frames that were flat to within 0.5%.

b) Photometric Calibrations

Photometric calibration was provided by observations of red-blue pairs of standard stars selected from the list of

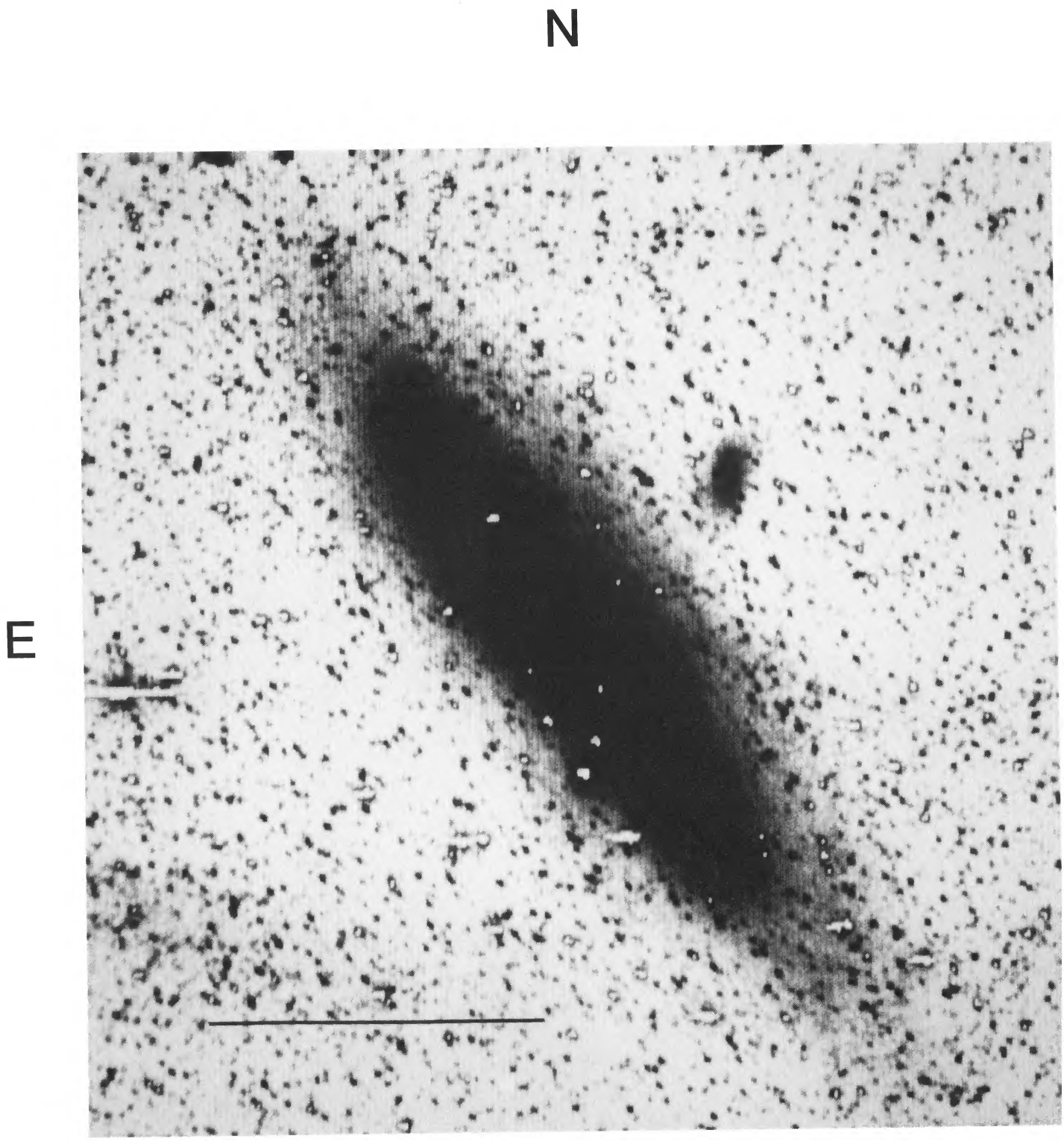

FIG. 2.—The *R* band CCD image of M31 taken with the 1 inch telescope. Image scale is $\sim 30''$ pixel^{-1}. Bar indicates one degree. This image is 2°.9 on each side.

Landolt (1983). Typically two to three pairs were observed over the range of one to two air masses each night. Photometric solutions were obtained by assuming that color terms were constant throughout each observing run and allowing for night-to-night variations in the extinction and zero points (Harris, Fitzgerald, and Reed 1981). Single measurement residuals (1 σ) were found to be typically 0.03 mag for the B bandpass and 0.02 for R and I. The color coefficients were relatively small (0.15 for B vs. $B-R$, and a few percent for R and I) and appear very stable over several observing runs ($\pm 10\%$).

The large pixels of the 1 inch telescope (30″) necessitated the use of bright standards ($m_v \approx 3$) in order to minimize contamination from nearby stars. Unfortunately, the Kron-Cousins and Landolt standards are much too faint. Our solution was to use the Johnson *UBVRI* standards given annually in *The Astronomical Almanac* and the transformations given by Fernie (1983) to convert the Johnson R magnitudes into Kron-Cousins R magnitudes. The transformations are claimed to be accurate to ~ 0.02 mag and thus sufficiently accurate for our purposes. The photometric solutions were then derived by the method previously outlined. Residuals for the 1 inch data were slightly higher (~ 0.04 for the B band and 0.02–0.03 for R). Color terms were similar.

c) *Total Magnitudes and Inclinations*

Accurate surface photometry of the galaxies was made possible by the GASP (GAlaxy Surface Photometry) software written by Mike Cawson (see Davis *et al.* 1985). Only a cursory description of the photometric procedures will be given here. A more detailed treatment will be given at a later date (Pierce 1988). In the context of the TF relations we will be concerned only with the calculation of total magnitudes and the determination of accurate inclinations through the fitting of ellipses to galaxy isophotes.

The wide field of view afforded by our instrumental configurations allowed a full growth curve to be obtained for each galaxy. The procedure was as follows. Stars and "bad pixels" were identified automatically, and the contaminated regions checked and edited on an image display system. An appropriate axial ratio for each galaxy was then measured from a contour plot, and the value was used by an aperture photometry program to construct elliptical annuli outward from the galaxy's central position at 1 pixel intervals. The intensity within each annulus was calculated and a running sum updated. The result was a photometric growth curve of the intensity within a given radius as a function of radius. Contaminated pixels were replaced with the average of the pixels within the annulus containing the contaminated pixels. A small number of galaxies were found to extend beyond the image boundaries. In these cases the "missing" pixels were replaced with the average of the portion of the annulus on the frame. This extrapolation introduces additional uncertainty in the magnitudes for these objects, but we estimate the uncertainty should be less than 0.1 mag since the regions not sampled are at very low surface brightness levels. These objects are indicated in Table 1. The sky level for each field was estimated from the mode of the pixel values of the entire CCD frame. The mode of the histogram will only be slightly biased by the presence of the galaxy. Nevertheless, small adjustments in the sky level ($\leq 1\%$) were often necessary to force the growth curves to become flat. The total intensity was then directly measured. The uncertainty in the total magnitudes introduced by the uncertainty in the sky adjustments should be only 2%–3%. In any event, we feel that this is the most objective way to determine the total magnitude of a galaxy.

The apparent magnitudes were then corrected for internal and Galactic extinction. The internal extinction was corrected only to face-on orientation as outlined by Tully and Fouqué (1985). No trends of TF residuals with color or with inclination were found, suggesting that these corrections are appropriate. This matter will be discussed more fully at a later date (Pierce 1988). The corrections for Galactic extinction (Burstein and Heiles 1978) are very small for the cluster sample but are substantial for the local calibrators (0.2 mag at B for M31). The extinctions in the R, I, and H bands were assumed to be 61%, 44%, and 10% of the extinction for the B band. These values were derived by applying van de Hulst's parameterization of the Whitford reddening law (see Johnson 1968) for Johnson bandpasses and then transforming to the Kron-Cousins bandpasses (Fernie 1983).

The inclinations were calculated from axial ratios assuming an intrinsic ratio of 0.2 (the axial ratio for an edge-on system) in the standard way (e.g., Holmberg 1958) but with one important difference. Rather than simply measuring the axial ratio at a particular isophote we prefer to fit ellipses to the isophotes of the galaxy and obtain the axial ratio as a function of radius (and surface brightness). We then determine a characteristic axial ratio over the range in radius (surface brightness) dominated by the disk. An estimate of the errors in our inclinations is 3°. The mean difference and dispersion between our inclinations and those quoted in the *Nearby Galaxies Catalog* (Tully 1987) is $0° \pm 7°$ (rms). The rms difference is basically a measure of the error in previous inclination determinations. Note that the sample selection requiring that inclinations be $\geq 30°$ was based on inclinations from the *Nearby Galaxies Catalog* and not the CCD data.

We have found that a significant morphological-type dependence can be generated if inclinations are derived from simply the axial ratio at a specific isophote. For late-type galaxies the disk dominates over a wide range of radii, while for early-type systems the bulge/halo can dominate at both small and large radii. We believe that our method of ellipse fitting results in inclinations that are less sensitive to systematic effects. A detailed discussion of this point will be deferred (Pierce 1988). The corrected total magnitudes are presented along with the inclinations and extinction corrections in Table 1. We also present H magnitudes for the galaxies in Table 1 when available (Aaronson *et al.* 1982*b*).

d) H I *21 Centimeter Data*

H I 20% peak intensity line widths were obtained from several sources (Fisher and Tully 1981; Helou *et al.* 1981; Appleton and Davies 1983; Giovanelli and Haynes 1983; Helou, Hoffman, and Salpeter 1984; Schwarz 1985; Warmels 1986; Hoffman *et al.* 1987). A systematic correction of 5% was subtracted from the line widths measured from the profiles given by Warmels (1986). In cases where there was more than one source for a galaxy we computed a weighted average. The differences in line widths in these cases were ± 11 km s^{-1} (rms). The line widths were then corrected for inclination and the effects of random motions as outlined by Tully and Fouqué (1985) using the inclinations we obtained through ellipse fitting. The H I information is included in Table 1.

TABLE 1

CLUSTER DATA

Galaxy (1)	Type (2)	$B_T^{b,i}$ (3)	$R_T^{b,i}$ (4)	$I_T^{b,i}$ (5)	$H_{-0.5}^{b,i}$ (6)	A_B (7)	i (8)	W_{20} (9)	log W_R^i (10)	Sources (11)
				Virgo Cluster						
NGC 4178	8B	11.47	10.69	10.32	10.09	0.61	78	284	2.401	1, 2
NGC 4189	6X	12.34	11.25	10.75	...	0.22	55	286	2.492	3, 6
NGC 4192*	2X	10.24	9.13	8.61	7.69	0.79	86	475	2.641	3
NGC 4206	4A	12.18	11.28	10.93	10.27	0.71	90	290	2.401	1, 2, 3, 6
NGC 4212	4A	11.69	10.46	10.04	...	0.19	44	282	2.566	3
NGC 4216*	3X	10.12	8.83	8.34	7.26	0.72	90	537	2.698	1, 2, 6
NGC 4254	5A	10.28	9.26	8.81	...	0.11	29	268	2.712	1, 2, 6
NGC 4321*	4X	9.91	8.76	8.19	...	0.07	25	273	2.784	1, 2, 6
NGC 4380	2A	12.23	10.89	10.23	9.76	0.23	61	303	2.489	3
NGC 4388	3P	11.05	10.06	9.62	8.78	0.77	83	375	2.531	1, 2, 6
NGC 4450	2A	10.81	9.44	8.82	8.03	0.16	48	324	2.600	1, 2, 3
NGC 4451	5	13.27	12.07	11.55	...	0.14	51	236	2.425	5
NGC 4498	7B	12.62	11.63	11.11	10.73	0.29	63	200	2.274	1, 2, 3, 6
NGC 4501	3A	10.07	8.82	8.18	7.10	0.31	61	541	2.764	1, 2, 3, 6
NGC 4519	7B	12.47	11.59	11.14	10.73	0.09	44	197	2.391	1, 3, 6
NGC 4522	4	12.47	11.58	11.11	10.53	0.65	79	245	2.326	2, 3
NGC 4532	10B	12.11	11.32	10.94	10.39	0.23	61	230	2.352	1, 3
NGC 4535	5X	10.58	9.55	9.09	8.44	0.10	45	289	2.569	1, 2, 3, 6
NGC 4548	3B	10.87	9.52	8.89	...	0.12	35	261	2.620	1, 2, 6
NGC 4571	6A	11.96	10.63	10.01	...	0.11	35	175	2.427	1, 2, 3, 6
NGC 4579	3X	10.30	8.93	8.33	...	0.18	42	377	2.720	1, 2
NGC 4639	3X	12.17	10.95	10.39	...	0.22	55	303	2.521	1, 6
NGC 4647	5X	11.87	10.72	10.20	...	0.13	40	198	2.431	3, 6
NGC 4651	5A	11.26	10.13	9.60	8.62	0.20	55	384	2.634	1, 6
NGC 4654	6X	10.84	9.87	9.41	8.76	0.27	58	307	2.511	1, 2, 6
NGC 4689	5A	11.73	10.49	9.89	...	0.11	39	205	2.459	3, 6
NGC 4698	2A	11.39	9.92	9.33	8.36	0.24	62	455	2.679	1, 3, 6
UGC 7209	4A	13.39	12.34	11.82	...	0.14	49	261	2.490	3
UGC 7249	10	15.17	14.51	14.28	...	0.54	74	121	2.083	5
UGC 7279	9	14.27	13.63	13.20	...	0.68	90	248	2.324	1
UGC 7352	8	14.31	13.51	13.30	...	0.19	57	188	2.272	5
UGC 7513	5	13.04	12.03	11.50	10.67	0.67	90	298	2.415	1, 2
UGC 7547	10	15.22	14.51	14.07	...	0.21	53	89	1.944	1, 4
UGC 7822	10	14.34	13.68	13.36	...	0.23	61	138	2.100	4
				Ursa Major Cluster						
NGC 3726	5X	10.70	9.74	9.23	8.87	0.16	53	291	2.534	1, 7
NGC 3729	1BP	12.24	10.91	10.29	...	0.12	48	280	2.528	8
NGC 3782	6XP	13.16	12.40	11.99	11.70	0.08	38	140	2.265	1, 7
NGC 3877	5A	11.10	10.06	9.52	8.63	0.68	86	364	2.491	1
NGC 3893	5X	11.04	9.98	9.57	8.77	0.16	54	308	2.535	1, 7
NGC 3917	6A	11.98	10.97	10.49	9.99	0.67	82	279	2.387	1
NGC 3949	4A	11.45	10.49	10.13	9.44	0.15	53	280	2.496	1, 7
NGC 3953	5B	10.77	9.47	8.80	7.93	0.24	62	418	2.649	1, 7
NGC 3972	4A	12.50	11.51	11.03	10.43	0.61	78	268	2.371	1, 7
NGC 4010	9	12.59	11.68	11.18	10.41	0.67	90	276	2.377	1, 7
NGC 4013	4	11.59	10.31	9.66	8.48	0.67	85	398	2.559	1
NGC 4051	4X	10.94	9.76	9.25	...	0.05	35	267	2.631	1
NGC 4088	5XP	10.88	9.75	9.29	8.41	0.42	71	376	2.548	1, 7
NGC 4100	5A	11.38	10.26	9.71	8.82	0.62	77	424	2.594	1, 7
NGC 4102	3X	11.91	10.48	9.91	...	0.17	55	327	2.537	1, 7
NGC 4157	3X	11.47	10.17	9.58	8.28	0.69	90	421	2.583	1, 7
NGC 4183	6A	12.33	11.64	11.21	10.60	0.67	90	251	2.328	1
NGC 4217	3	11.41	10.11	9.39	8.59	0.61	78	421	2.593	1
UGC 6446	7A	13.56	12.82	12.44	...	0.14	51	157	2.220	1
UGC 6667	5	13.70	12.76	12.27	12.07	0.67	90	198	2.210	1, 7
UGC 6816	10B	14.21	13.52	13.28	...	0.14	51	140	2.164	1
UGC 6917	10	13.09	12.07	11.32	...	0.18	55	201	2.330	1
UGC 6923	10	13.59	12.78	12.28	12.03	0.36	69	170	2.170	1, 7
UGC 6930	7X	12.71	11.71	11.16	...	0.06	33	137	2.338	1, 7
UGC 6983	6B	13.17	12.32	11.94	11.66	0.17	55	197	2.307	1, 7
UGC 7218	10P	14.74	13.91	13.53	...	0.23	61	111	2.004	1, 7

NOTES.—Notation is generally the same as that found in the Nearby Galaxies Catalog (Tully 1987). Col. (1): An asterisk denotes extrapolation off the image boundaries was necessary in constructing the growth curve. Col. (2): Numeric type code runs from 1 = Sa to 10 = Im. B denotes bar, A denotes nonbar, X denotes intermediate case. P denotes peculiarity. Cols (3)–(5): B_T, R_T, I_T are total apparent magnitudes. Cols (3)–(6): Superscript b implies correction applied for Galactic extinction. Col. (6): $H_{-0.5}$ is an aperture magnitude. Col. (7): A_B is sum of Galactic and inclination extinction corrections in B band. Col. (8): i denotes inclination. Col. (9): W_{20} is H I profile width at 20% of maximum intensity. Col. (10): W_R^i is width corresponding statisically to $2V_{max}$. Superscript i implies inclination correction applied. Col. (11): Sources for W_{20} are (1) Tully 1987; (2) Giovanelli and Haynes 1983; (3) Helou, Hoffman, and Salpeter 1984; (4) Hoffman *et al.* 1987; (5) Hoffman 1987; (6) Warmels 1986; (7) Appleton and Davies 1982; (8) Schwarz 1985.

III. LUMINOSITY–LINE-WIDTH RELATIONS FOR THE URSA MAJOR AND VIRGO CLUSTERS

a) The Data

The *B*, *R*, *I*, and *H* TF relations for the Ursa Major and Virgo clusters are presented in Figure 3. The most obvious features of the diagrams are (1) the greater dispersion in Virgo compared with Ursa Major, (2) the increase in slope going from the *B* to the *H* bandpass, and (3) the lower dispersion in the *R*, *I*, and *H* bands when compared to the *B* band, particularly for the Ursa Major Cluster.

Accidentally, the Ursa Major and Virgo Clusters turn out to be at essentially the same distance. Data from the two clusters are superposed in Figure 4. The results of linear least-squares fits to the combined data sets are superposed on the figure.[2] We fitted to the combined data set to maximize the domain of relevance, since the Ursa Major Cluster lacks galaxies as luminous as the brightest in Virgo and since the Virgo Cluster has been poorly sampled at low luminosities because of incompletion in our observing program. The solid line is the double regression fit, and the dashed line is the fit derived assuming errors in line width only. It will be explained further along why the latter fit is of interest to us.

The results of the fits are recorded in Table 2. The slopes are derived from the combined data set. Slopes determined for the two clusters separately are never significantly different. The scatter is less with the Ursa Major sample, however. An rms dispersion characteristic of the *R*, *I*, and *H* bands is 0.30 mag.

b) Intrinsic Scatter in the Luminosity–Line-Width Relations

The observed dispersions in the TF relations for the Ursa Major members is a combination of the intrinsic dispersions of the relationships, measurement uncertainties, and the depth of the cluster. The Ursa Major Cluster occupies an elliptical region on the sky 15° × 11° with the major axis aligned with the plane of the Local Supercluster. The line of sight also lies in

[2] The analysis excludes UGC 7209, UGC 7279, and UGC 7352, as these galaxies are almost certainly in the background of the Virgo Cluster. The velocities and inferred distances for these three galaxies are consistent with them being at about twice the Virgo distance (see § IIIc) and in the proximity of the Virgo W Cluster (de Vaucouleurs 1961) or in what Ftaclas, Fanelli, and Struble (1984) call the M cloud.

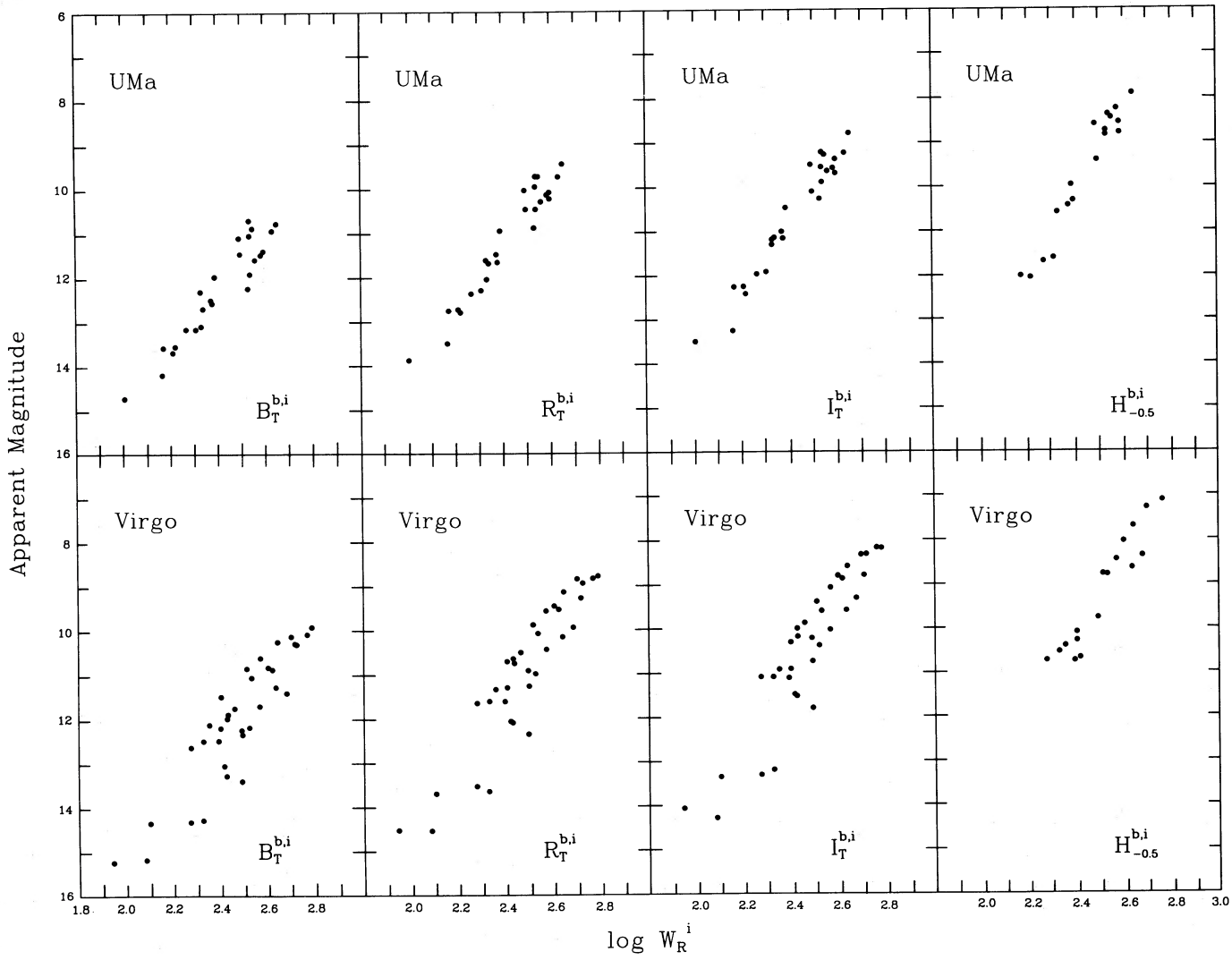

FIG. 3.—The luminosity–line-width relations for the Ursa Major Cluster (*top panel*) and Virgo Cluster (*bottom*). The *B*, *R*, and *I* band photometry is from our CCD photometry program, while the *H* band data is from Aaronson *et al.* (1982*b*).

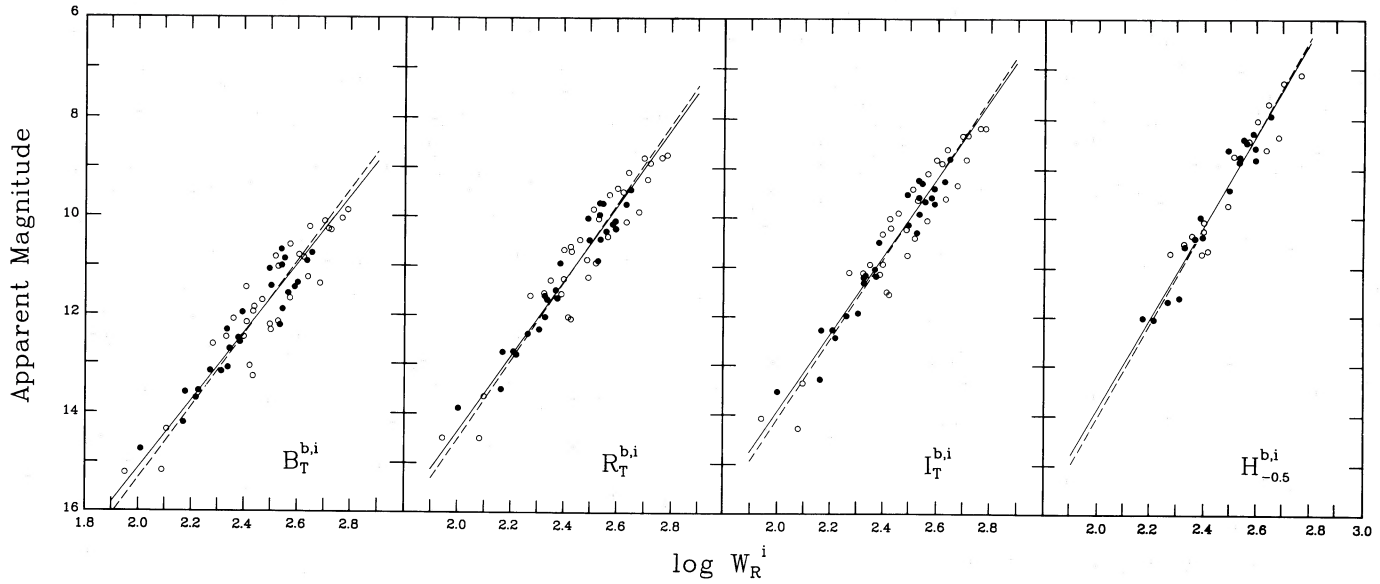

FIG. 4—Luminosity–line-width relations for the Virgo and Ursa Major clusters combined (three background galaxies from the Virgo field are eliminated). Ursa Major data are represented by solid points, and Virgo data are represented by open circles. Solid line represents a double-regression least-squares fit, while dashed line is a fit minimizing the dispersion in the line-width dimension.

the plane of the Local Supercluster. The expected depth of the cluster is roughly the observed major axis dimension of the cluster, which translates to ± 0.17 mag rms. Hence, the intrinsic plus measurement dispersion of the TF relations is expected to be only ~ 0.25 mag or $\sim 12\%$ in distance. This dispersion is considerably smaller than values that are usually quoted (Tully and Fisher 1977; Aaronson, Huchra, and Mould 1979; Visvanathan 1983; see Sandage 1988 for a higher value). Some of this improvement can be attributed to accurate CCD photometry. However, more important is the greater accuracy of the inclinations we derive through ellipse fitting over those obtained from axial ratios measured at a single isophote on a photograph. Improved inclinations lead to significantly improved deprojected line widths.

It is noted that in the various TF diagrams the displacement of individual galaxies from the mean relations is highly correlated between bandpasses (Visvanathan 1981*a*). Correlation can be due to depth effects, errors in line width (either in measurements or deprojections), and intrinsic mass-to-luminosity variations. Scatter orthogonal to the correlation can be due to errors in magnitudes (either in measurements or extinctions) and intrinsic population variations. The observed orthogonal scatter, given by differential distance modulus estimates, is 0.11 mag (rms) between *R* and *I* and 0.21 mag (rms) between *B* and *I*. The increased scatter between *B* and *I* must mainly be due to intrinsic variations related to star formation, and much of the (very modest) *R* to *I* scatter must be attributed to the same cause. If the observed orthogonal scatter (0.11) and the inferred distance scatter (0.17) are subtracted in quadrature from the total observed scatter (~ 0.30), then the scatter attributable to line width errors and intrinsic variations in the distribution of mass versus light is ~ 0.22 mag. Bothun and Mould (1987) estimate that errors in line width (due to measurement plus inclination corrections) correspond to ~ 0.18 mag. Evidently, there is very little room for intrinsic mass-to-light or population variations. However, there must be *some* intrinsic scatter, because of the slight correlations with type reported in the next paragraph.

TABLE 2

LEAST-SQUARE FITS TO THE COMBINED TF RELATIONS

Bandpass	Slope (errors in W)	Slope (double regression)	σ (Virgo)	σ (UMa)
$B_T^{b,i}$	-7.30 ± 0.32	-6.86 ± 0.32	0.50	0.37
$R_T^{b,i}$	-7.97 ± 0.29	-7.64 ± 0.29	0.47	0.31
$I_T^{b,i}$	-8.16 ± 0.29	-7.85 ± 0.29	0.48	0.28
$H_{-0.5}^{b,i}$	-9.59 ± 0.43	-9.25 ± 0.43	0.40	0.31

Roberts (1978) and Rubin *et al.* (1985) have suggested that a strong morphological-type dependence is present, in that earlier morphological types are fainter at a given line width than later morphological types. A slight effect of this nature is seen in the combined Virgo and Ursa Major samples in Figure 5. If the slopes of the TF relations are fixed at the values found for the combined samples, we can look for offsets in zero point as a function of type. In the *B* band, early types (Sa–Sb) are fainter by 0.23 mag (2.1 σ) and late types (Sd–Im) are brighter by 0.14 mag (1.4 σ). At the *R*, *I*, and *H* bands the corresponding shifts are 0.07–0.11 mag and the significance levels are $\sim 1\ \sigma$. On this point, we concur with Aaronson and Mould (1983) and Visvanathan (1983) that type dependencies are second-order effects of marginal significance at the near-infrared passbands. Strong type dependency effects can be an artifact of samples that are not representative of a complete sample, as the Rubin *et al.* (1985) sample definitely is not.

Incidently, Aaronson and Mould (1983) found evidence for curvature in the TF relation. As Bottinelli *et al.* (1984) points out, such an effect could be an artifact of the line-width definition. Our W_R^i line widths (Tully and Fouqué 1985) are statistically equivalent to twice the maximum rotation velocity. We find no evidence for curvature in the relationships plotted with this parameter.

Giraud (1987) has suggested that the use of aperture magnitudes results in a slightly smaller dispersion for the TF relations than the use of total magnitudes. We have constructed

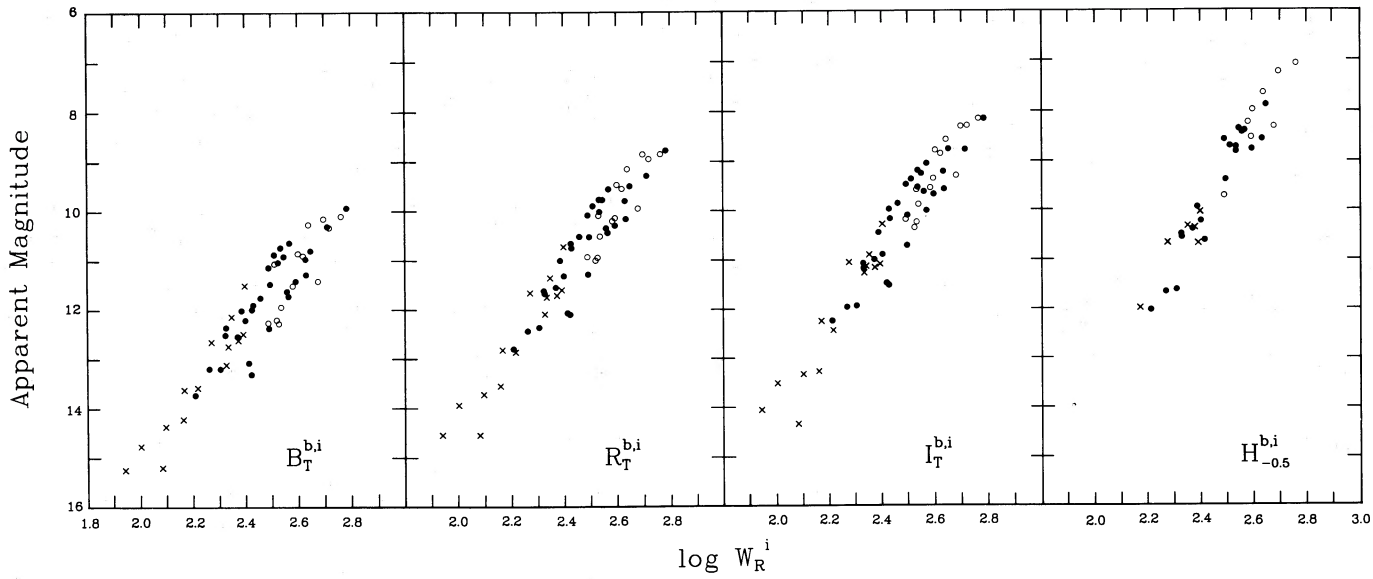

FIG. 5.—Type dependencies in the luminosity–line-width relationships with the combined clusters sample. *Open circles*: types Sa-Sb. *Solid points*: types Sbc-Scd *Crosses*: types Sd-Im.

aperture magnitudes (see § III*d*) from our growth curves and find the dispersion to be *higher* with aperture magnitudes than with total magnitudes (0.4 mag rms vs. 0.3 mag). An examination of the growth curves indicates that the aperture magnitude (at $\sim D_{25}^{b,i}/3$) is rather unstable, especially at shorter wavelengths, as in this region the growth curve is often rapidly rising.

Given the evidence for *some* type dependencies, especially in the *B*-band, presumably a distance estimator with even less scatter could be devised through the inclusion of another parameter, albeit at the cost of added complexity.

c) Possible Projection Contamination in the Virgo Cluster

The scatter associated with the Virgo sample is 0.47 mag in the near-infrared passbands, compared with 0.30 mag for the Ursa Major sample. If the intrinsic plus measurement scatter is 0.25 mag, as we concluded in the previous section, then there is "excess" scatter associated with the Virgo sample of $\sim$0.40 mag. This amount is considerably in excess of the scatter expected from the depth effect within the 6° cluster of $\sim$0.14 mag.

There are two possibilities: (1) the intrinsic scatter is greater because of environmental influences in the Virgo Cluster or (2) a substantial number of the spiral galaxies viewed in projection against the 6° Virgo Cluster are infalling toward the cluster but are not yet within the cluster.

There has been considerable discussion of the first point (see Haynes and Giovanelli 1986 for a recent summary). There is now a general consensus that the cluster environment affects the H I content of galaxies. On the other hand, Guhathakurta *et al.* (1987) have mapped the H I in a number of Virgo Cluster spirals and find that all but NGC 4438 and NGC 4569 have H I that extend to beyond the turnover point of their rotation curves. Thus environmental influence on the line widths is unlikely in general.

Regarding the second point, Tully and Shaya (1984) have shown that there are galaxies just outside the 6° boundary of the cluster that are surely infalling and, indeed, will enter the cluster in 1–3 Gyr. There is a prominent group beyond Virgo with negative velocities with respect to the cluster and a small number of galaxies in front of Virgo with positive velocities with respect to the cluster. It could well be that there are galaxies associated with these infalling groups but projected against the cluster and, hence, impossible to identify without sensitive distance information.

It turns out that the galaxies with the most discordant distances in the Virgo sample have the distance-velocity signature expected from an infalling population. Distance estimates to individual galaxies in the sample are listed in Table 3 and are plotted in Figure 6. The distance scale is set by the zero-point calibration discussed in § IV*c*, but it is only *relative* distances that concern us here. The curves illustrate velocities that infalling galaxies would have at two representative projected angles with respect to the center of the cluster according to the model discussed by Tully and Shaya (1984). The vertical lines indicate the 1 σ distance limits if the scatter (intrinsic plus depth) is represented by the Ursa Major sample (0.30 mag). Assuming the Ursa Major scatter, roughly nine galaxies in a sample of 31 would be expected to deviate by greater than 15% from the mean Virgo distance, whereas 20 are observed. As was already pointed out, infalling galaxies from the near side of the cluster should have high velocities and infalling galaxies from the far side should have low velocities. Of the 20 galaxies most discordant in distance, only four have velocities incompatible with infall. We speculate that roughly half of the 20 are indeed infalling and are seen in projection against the cluster.

Whether one accepts that the intrinsic scatter in the Virgo sample is greater than in Ursa Major or accepts the viewpoint that it is at least plausible that there are infalling galaxies that should not be considered part of the cluster, we will arrive in § IV*c* at essentially the same conclusion regarding the Virgo distance.

d) Slope Variations with Wavelength

There has been considerable discussion in the literature regarding the slope of the *B* band TF relation. Estimates have spanned a range of almost a factor of 3 (see Bottinelli *et al.* 1980; Burstein *et al.* 1982). It is clearly important to compare

TABLE 3

VIRGO CLUSTER MEMBERSHIP AND VELOCITIES

Galaxy	Velocity (km s^{-1})	Distance[a]	Distance/Velocity[b]
NGC 4178	285	12.7	−/−
NGC 4189	2039	21.2	+/+
NGC 4192	−220	13.5	−/−
NGC 4206	616	15.9	*
NGC 4212	−163	19.5	+/−
NGC 4216	55	14.5	*
NGC 4254	2323	18.0	*
NGC 4321	1522	18.4	*
NGC 4380	872	18.2	*
NGC 4388	2527	14.1	*
NGC 4450	1899	13.6	−/+
NGC 4451	600	24.8	+/−
NGC 4498	1448	11.8	−/+
NGC 4501	2217	17.8	*
NGC 4519	1136	17.8	*
NGC 4522	2241	13.6	−/+
NGC 4532	1909	13.5	−/+
NGC 4535	1873	13.2	−/+
NGC 4548	406	15.1	*
NGC 4571	282	12.9	−/−
NGC 4579	1729	16.3	*
NGC 4639	917	20.6	+/−
NGC 4647	1285	13.5	−/+
NGC 4651	748	20.7	+/−
NGC 4654	978	12.2	−/0
NGC 4689	1715	13.4	−/+
NGC 4698	905	22.6	+/−
UGC 7209	2144	34.4	Bkg
UGC 7249	541	22.7	+/−
UGC 7279	1883	33.8	Bkg
UGC 7352	2363	28.1	Bkg
UGC 7513	898	22.3	+/−
UGC 7547	1016	13.8	−/0
UGC 7822	1995	16.3	*

[a] Distance from double regression relationships weighted $B=0.19$; $R=0.31$; $I=0.19$; $H=0.31$; in Mpc.

[b] Asterisk denotes galaxy within 1 σ of mean distance; Bkg = at roughly twice the distance of the Virgo Cluster; +/(or −/) is distance greater (or less) than mean by ≥ 1 σ; /+(or /−) is velocity greater (or less) than mean by ≥ 1 σ; /0 = velocity within 1 σ of mean.

slopes derived in the same manner. Moreover it is generally appreciated that the slope depends on wavelength (Visvanathan 1981*a*; Tully, Mould, and Aaronson 1982; Bottinelli *et al.* 1983).

In Figure 7 we present the double-regression slope of the TF relation as a function of wavelength in our systems. The solid points are the slopes for the combined cluster sample obtained from our CCD total magnitudes. In contrast, the open points correspond to the slopes derived from aperture magnitudes, with apertures related to the apparent size of the galaxies.[3] This procedure has been standard for H band photometry. With our complete growth curves for all the galaxies it is trivial to derive magnitudes for an equivalent size aperture in the other photometric bands.

It is seen in Figure 7 that the aperture magnitude slopes are steeper. In hindsight, the reason is obvious. Given the diminished central concentration in lower luminosity galaxies, an aperture of a given fractional size of an isophotal level will contain a proportionately smaller fraction of the intensity of a galaxy of lower luminosity. The diminishing central concentration is related to the decrease in the bulge/disk ratio with decreasing luminosity.

Evidently, with total magnitudes the slope of the TF relation is asymptotically approaching a constant value of ~ 8.0 toward longer wavelengths. The decrease in slope toward shorter wavelengths is interpreted as being primarily due to the decrease in mean age of the stellar populations in low-luminosity systems (lower luminosity systems are bluer) and secondarily due to diminished metallicity and/or a flatter initial mass function in low-luminosity systems (Visvanathan 1981*b*; Tully, Mould, and Aaronson 1982).

In detail, the slope depends on a couple of other things. It depends on the definition of the line-width parameter, and our parameter, $W^i_R \approx 2V_{\max}$, is more physically meaningful than the 20% full-intensity line width from which it is derived (Tully and Fouqué 1985). It also depends on the fitting procedure. We use an equal weight double regression.

The asymptotic value of the slope of 8.0 implies $L \propto V^{3.2}_{\max}$. The familiar result that $L \propto V^4$ (Aaronson, Huchra, and Mould 1979) seems to be an artifact of an aribtrary choice of aperture.

IV. LOCAL CALIBRATION AND CLUSTER DISTANCES

a) Local Calibration of the Luminosity–Line-Width Relations

Three relevant nearby galaxies have distances derived from studies of Cepheid and RR Lyrae variables: M31, M33, and NGC 2403. The accepted distances for these galaxies and the various method used to derive them are summarized in Table 4. These results were placed on a common scale by the assump-

[3] Specifically the aperture size (A) is chosen such that $\log(A/D^{bi}_{25}) = -0.5$, where D^{bi}_{25} is the diameter of the B-band 25 mag arcsec^{-2} isophote, corrected for extinction and projection.

TABLE 4

DATA FOR LOCAL GALAXIES

Galaxy (1)	Distance Modulus (2)	$M^{b,i}_B$ (3)	$M^{b,i}_R$ (4)	$M^{b,i}_I$ (5)	$M^{b,i}_H$ (6)	A_B (7)	i (8)	W_{20} (9)	log W^i_R (10)	Sources (11)
NGC 224	24.4	−20.57	−21.71	...	−23.54	0.80	78	535	2.706	1, 2
NGC 598	24.2	−18.09	−18.96	...	−19.84	0.34	58	204	2.305	3, 4
NGC 2403	27.5	−19.08	−19.90	−20.27	−21.07	0.39	57	257	2.412	5, 6

NOTES.—Notation is generally the same as that found in the Nearby Galaxies Catalog (Tully 1987). Col. (3)–(5): $m^{b,i}_B$, $M^{b,i}_R$, and $M^{b,i}_I$ are total absolute magnitudes. Cols. (3)–(6): Superscript b denotes correction applied for Galactic extinction. Superscipt i denotes inclination correction applied. (Col. (6): $M^{b,i}_H$ denotes an aperture magnitude. Col (7): A_B denotes sum of Galactic and inclination extinction corrections in B band. Col (8): i denotes inclination. Col. (9): W_{20} is H I profile width at 20% of maximum intensity. Col. (10): W^i_R is width corresponding statistically to $2V_{\max}$. Superscript i denotes inclination correction applied. Col. (11): Sources for Distance Moduli are (1) Welch *et al.* 1986; (2) Pritchet and van den Bergh 1987; (3) Christian and Schommer 1987; (4) Freedman 1985; (5) Tammann and Sandage 1968; (6) Freedman 1987.

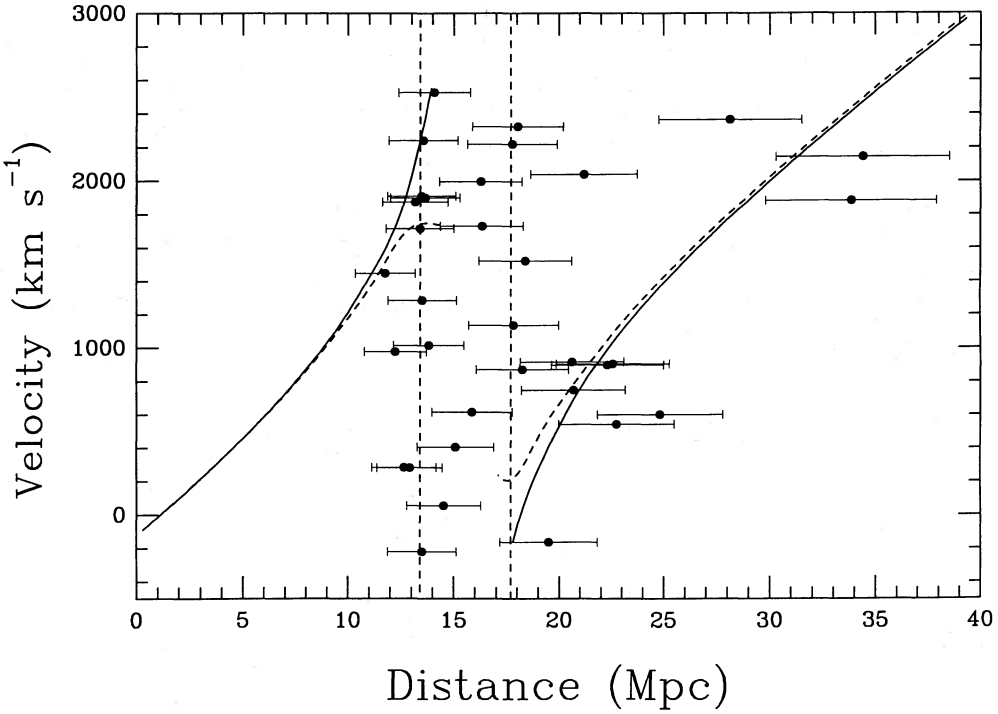

FIG. 6.—Velocity vs. distance for galaxies in the Virgo Cluster sample. The vertical dashed lines correspond to ± 0.30 mag limits to the cluster. A galaxy outside of the cluster but viewed in projection 1° from the center of the cluster is predicted to lie on the locus described by the solid line by the Tully and Shaya infall model. A galaxy viewed in projection 6° from the center of the cluster would be on the dashed curve. The three far-background galaxies are in the neighborhood of the Virgo W Cluster.

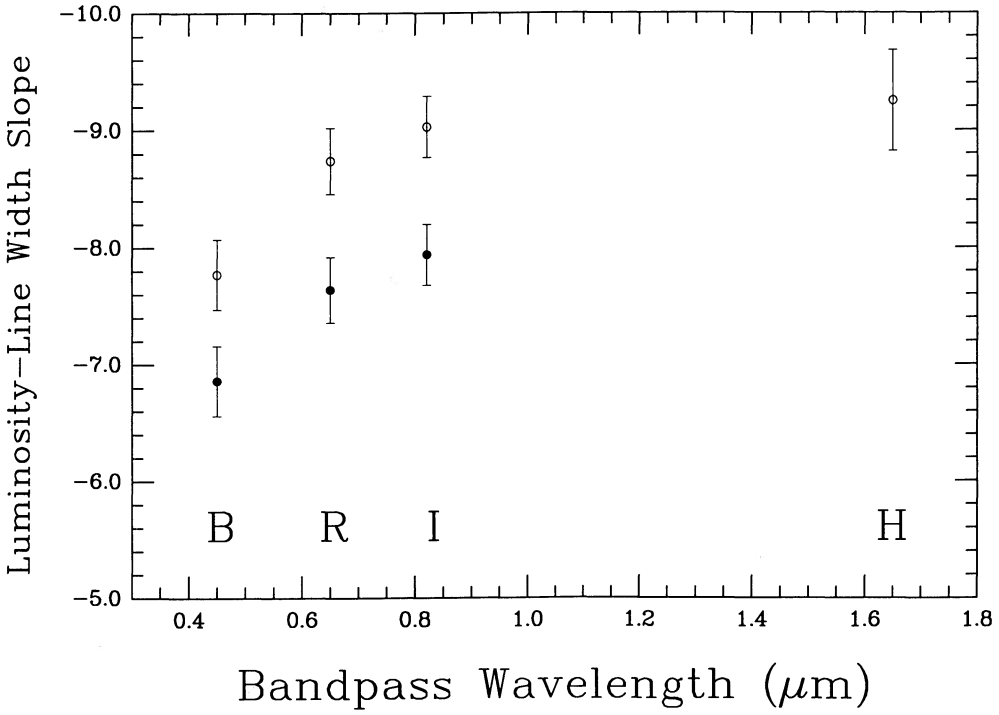

FIG. 7.—The dependence of the slope of the luminosity–line-width relation on wavelength. Solid points are the slopes derived from total or asymptotic magnitudes, while open points are from aperture magnitudes where $\log (A/D) = -0.5$.

tion that the Large Magellanic Cloud has a distance modulus of 18.6 (Welch *et al.* 1987).

The TF relation zero points for each bandpass were determined by constraining the slopes of the relations to be those found from the double-regression fits on the combined cluster sample and then minimizing the vertical dispersion of the calibrators about these lines. The resultant TF relations are

$$M_B^{b,i} = -6.86 \log W_R^i - 2.27 \pm 0.25 ,$$
$$M_R^{b,i} = -7.64 \log W_R^i - 1.28 \pm 0.14 ,$$
$$M_I^{b,i} = -7.94 \log W_R^i - 1.11 \pm 0.25 ,$$
$$M_H^{b,i} = -9.25 \log W_R^i + 1.40 \pm 0.14 .$$

The errors in the zero point are the dispersion measured for the Ursa Major members reduced by the assumed contribution due to the depth of the cluster of ± 0.17 mag and divided by $N^{1/2}$, where N is the number of calibrators. The I band zero point is determined solely by NGC 2403. An additional error of 0.15 mag has been added in quadrature in the case of the B band due to a possible systematic error in the zero point. This matter will be discussed in (§ IV*b*). The errors in the slopes were determined from the fits to the combined clusters sample and are given in Table 2.

b) Do the Local Calibrators have Normal Color–Line-Width Properties?

A test of the normalcy of the local calibrators is to compare them with the cluster systems in a distance independent plot such as a color–line-width diagram. The $B-R$ color–line-width relationship for our sample is shown in Figure 8. The solid points are the Ursa Major Cluster members, while the open circles are members of the Virgo Cluster. There is no significant difference in either the slope or the dispersion between the two cluster samples. We take this as evidence that there is no significant difference in the pertinent intrinsic properties of the Ursa Major and Virgo member galaxies. However, with respect to the mean, two of the three local calibrators (M31 and NGC 2403) lie significantly displaced toward bluer colors for their line widths. The number of local calibrators is obviously too small to draw any conclusions about differences in the stellar content between field galaxies and cluster members. However, with a mean blueward displacement of ~ 0.15 mag for the calibrators, we can expect the B-band distance calibration to differ from those of the R and I bands by a similar amount. As will be discussed in § IV*c*, this is just what we find. Given consistency between the near-infrared measurements for the calibrator systems and the generally increased scatter at the B band, we ascribe the added uncertainty to the B band.

c) Distances to the Ursa Major and Virgo Clusters

Distances to each cluster are computed in two ways, by (1) minimization of magnitude residuals in fits of the double-regression relationships and by (2) minimization of line-width residuals on the single regression relationships formed assuming errors in line width only. In addition, distances are derived separately for the entire Virgo sample and for the Virgo sample minus the five systems with distances that deviate by more than 2 σ (0.6 mag) from the mean that can be argued are infalling toward the cluster (all five have velocities

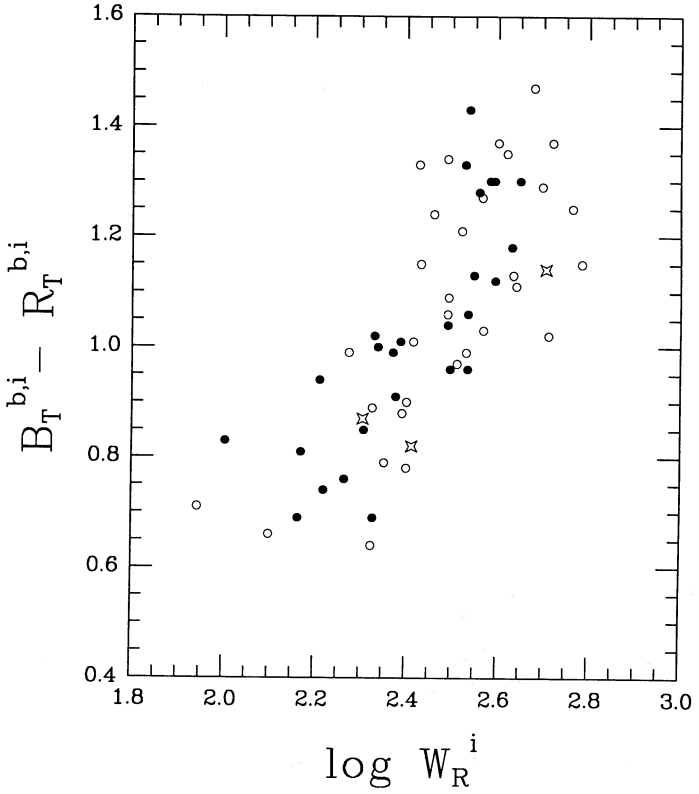

FIG. 8.—Color–line-width relationship. Filled circles represent Ursa Major members, the open circles represent Virgo members, and open stars represent the three local calibrators. It is noted that two of the local calibrators are rather blue for their line width.

TABLE 5

CLUSTER DISTANCE MODULI

Bandpass and Methods		UMa[a]	Virgo[b]	Virgo Core[c]	Error
B	Double regression	31.06	31.11	31.00	±0.26
	Regression on W_R	31.04	31.11	31.02	...
R	Double regression	30.93	30.97	30.87	±0.16
	regression on W_R	30.92	30.97	30.88	...
I	Double regression	30.96	31.06	30.96	±0.26
	Regression on W_R	30.96	31.07	30.98	...
H	Double regression	30.93	31.01	30.96	±0.17
	Regression on W_R	30.92	31.02	30.98	...

[a] Number of galaxies: 26; number in H band: 18.
[b] Number of galaxies: 31; number in H band: 17
[c] Number of galaxies: 26; number in H band: 14.

consistent with infall; see § IIIc). This limited Virgo sample will be referred to as the Virgo core subset.

The first method involves just the application of the relationships determined in § IVa. Given W^i_R, a distance modulus can be found for each member of a sample. Mean distance moduli for each sample are given in Table 5. Errors are predominantly (dispersion)/$N^{1/2}$ where N is the number of calibrators. Uncertainties in the distances of the calibrators are not included in this error budget.

The second method is employed to circumvent possible biases of the kind discussed by Teerikorpi (1987). With a magnitude-limited sample, there will be a tendency to include brighter galaxies and drop fainter galaxies at a line width roughly corresponding to the cutoff. Distances to galaxies near the magnitude limit will be underestimated and will pull the overall mean distance down. This bias is akin to the Malmquist bias suffered by a field sample. It is a dangerous bias if the intrinsic scatter of a relationship is large, and it is less of a problem if the intrinsic scatter is small.

Schechter (1980) showed that this bias is avoided by minimizing line width rather than magnitude residuals. The Virgo and Ursa Major clusters are close enough that essentially all candidates in these clusters can be detected in H I with a sufficient signal-to-noise ratio so that line-width measurements are not observationally biased. Consequently, a galaxy chosen on the basis of apparent magnitude can be assumed to be randomly drawn from the line-width distribution corresponding to the absolute magnitude of the system. The steeper regressions shown in Figure 4 (fits with uncertainties in line width) are the appropriate linear fits to the combined cluster samples. The horizontal shift of these relationships, that is, the minimization of the line-width residuals in fits to cluster and calibrator samples, gives the distance determination. The resultant distance estimates are included in Table 5. Error estimates are formally the same for the two methods. The fits based on this second method are illustrated in Figure 9.

There is no significant difference between the distance estimates derived by the two methods. The preferred distance to each cluster is the mean value derived by the line-width residual method, with a weight assigned to the determination provided by each passband that is inversely proportional to the error estimate (0.19, 0.31, 0.19, and 0.31 for the *B*, *R*, *I*, and *H* bands, respectively). Because of correlated errors between passbands, the errors in the mean distance estimates are not much less than the lowest error associated with the individual measurements.

Our final results are

$$(m - M)_{\rm UMa} = 30.95 \pm 0.16 \ (15.5 \pm 1.2 \ {\rm Mpc})$$

$$(m - M)_{\rm Vir} = 31.03 \pm 0.17 \ (16.1 \pm 1.3 \ {\rm Mpc})$$

$$(m - M)_{\rm Vir\,Core} = 30.96 \pm 0.20 \ (15.6 \pm 1.5 \ {\rm Mpc}) \, .$$

The difference in distance between the Virgo and the Virgo core samples arises because four of the five galaxies excluded by the 2 σ rejection criterion are apparently behind the cluster (see § IIIc). We will take the distance of the Virgo core sample as most representative of the distance to the cluster. The increased error takes into account the uncertainty associated with the specification of the core sample. Errors do not include uncertainties in the distances of the three local calibrators. Direct intercomparison of the TF diagrams for the two clusters indicates that the relative distances of the Virgo and Ursa Major clusters are the same to ±5% (rms).

V. MODEL OF THE VELOCITY FIELD AND H_0

a) *Local Supercluster Velocity Field*

The geometry of the Local Group, the Ursa Major Cluster, and the Virgo Cluster is shown in Figure 10. This is the view an observer would have when looking down onto the Supergalactic plane from the north Supergalactic pole. The relative geometry of the objects in this figure is well established, since the relative cluster distances are known with 5% accuracy and angles on the sky are well defined.

The question now is, how well are the velocities determined? To derive H_0 we want an estimate of what the velocities of the clusters would be in a freely expanding part of the universe. Hence, there are velocities that are observed and corrections to these velocities that are inferred.

Consider observed velocities first. We make the conventional correction to heliocentric velocities of 300 km s^{-1} toward $l = 90°$, $b = 0°$. The systemic velocity of the Ursa Major Cluster is well defined because the cluster dispersion is modest (148 km s^{-1}) and there is no apparent confusion: $V_0^{\rm UMa} = 967 \pm 20$ km s^{-1}. The situation with regard to the Virgo Cluster is more difficult, even though the problem has been studied in detail (e.g., de Vaucouleurs 1982; Huchra 1984; Binggeli, Tammann, and Sandage 1987). The velocity histogram for spirals is decidedly non-Gaussian, with evidence for substructure and, possibly, for recent and continuing infall. Moreover, there may be a contamination problem arising from galaxies associated with the Virgo W Cluster in the background. Given these caveats, we accept the systemic velocity determined by Binggeli, Tammann, and Sandage (1987) of $V_0^{\rm Vir} = 1016 \pm 42$ km s^{-1}.

Turn now to the more difficult question of non-Hubble motions. The velocity field of the Local Supercluster has been investigated by several groups (e.g., Aaronson *et al.* 1982*a*; Dressler 1984; Kraan-Korteweg 1984; Tammann and Sandage 1985; Aaronson *et al.* 1986; Lilje, Yahil, and Jones 1986). As a framework for the present discussion, we make use of the model of the Virgo Cluster region presented by Tully and Shaya (1984). This model is consistent with a retardation of the Galaxy by a Virgocentric mass distribution of $V_r^G = 300$ km s^{-1} (we attribute an uncertainty of ±100 km s^{-1}) and predicts agreement in the distances of the Ursa Major and Virgo clusters to within 1%. The model requires that the retardation of the Ursa Major Cluster by the mass at Virgo be roughly $V_r^{\rm UMa} = 370$ km s^{-1}. According to the model, an observer at

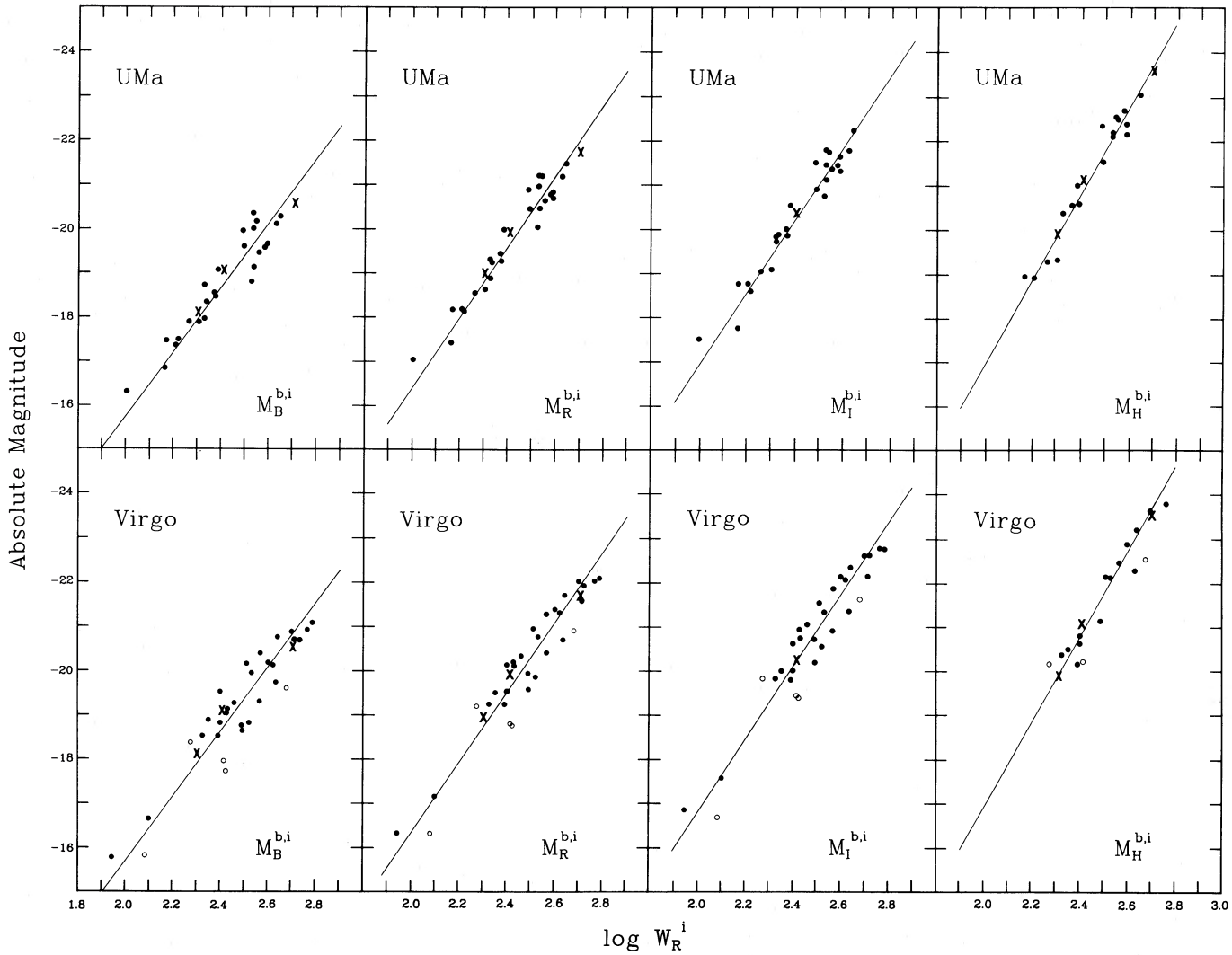

FIG. 9.—Luminosity–line-width relations on an absolute scale established by three nearby galaxies whose distances are reasonably well known: M31, NGC 2403, and M33. *Top panel*: Ursa Major Cluster. *Bottom panel:* Virgo Cluster. *Heavy crosses*: local calibrators. Open circles in the Virgo Cluster data are the galaxies with distances more than 2 σ from the mean and are excluded from the fit (Virgo core fit). The straight line is the single regression based on minimized residuals in line widths. *I* band data were not obtained for M31 or M33, so in this case the fit uses only NGC 2403.

rest in the Ursa Major Cluster would determine the Virgo Cluster systemic velocity to be $\sim$480 km s^{-1}. A summary of the observed and predicted velocities is provided in Table 6. The free expansion, or Hubble, velocities are given by

$$V_H^{Vir} = V_0^{Vir} + V_r^G$$

$$V_H^{UMa} = V_0^{UMa} + V_r^{UMa} \cos\phi + V_r^G \cos\theta$$

where $\phi = 71°$ and $\theta = 35°$. Since ϕ is close to 90°, V_H^{UMa} is relatively insensitive to V_r^{UMa}.

TABLE 6

OBSERVED AND INFERRED VELOCITIES

Velocity	Virgo	Ursa Major
Systemic	$V_0^{Vir} = 1016 \pm 42$ km s^{-1}	$V_0^{UMa} = 967 \pm 20$ km s^{-1}
Retardation	$V_r^G = 300 \pm 100$	$V_r^{UMa} = 370 \pm 100$
Rest Frame Uncertainty:	± 50	± 50
Hubble	$V_H^{Vir} = 1316 \pm 120$	$V_H^{UMa} = 1324 \pm 115$

There is additional uncertainty associated with local velocity components (Yahil, Tammann, and Sandage 1977; de Vaucouleurs, Peters, and Corwin 1977; Richter, Tammann, and Huchtmeier 1987). An estimate of this uncertainty is ± 50 km s^{-1}. There also could be components of motion, perhaps due to rotation or shear (Aaronson *et al.* 1982*a*; Lilje, Yahil, and Jones 1986) or other poorly explored manifestations of large-scale streaming (Dressler *et al* 1987). However, we are not able to assign a meaningful error estimate that encompasses these possibilities.

b) The Hubble Constant

An estimate of H_0 follows from our information on the two clusters. For Virgo,

$$H_0 = (1316 \pm 120)/(15.6 \pm 1.5) = 84 \pm 11 \text{ km s}^{-1} \text{ Mpc}^{-1} .$$

For the Ursa Major Cluster,

$$H_0 = (1324 \pm 115)/(15.5 \pm 1.2) = 85 \pm 10 \text{ km s}^{-1} \text{ Mpc}^{-1} .$$

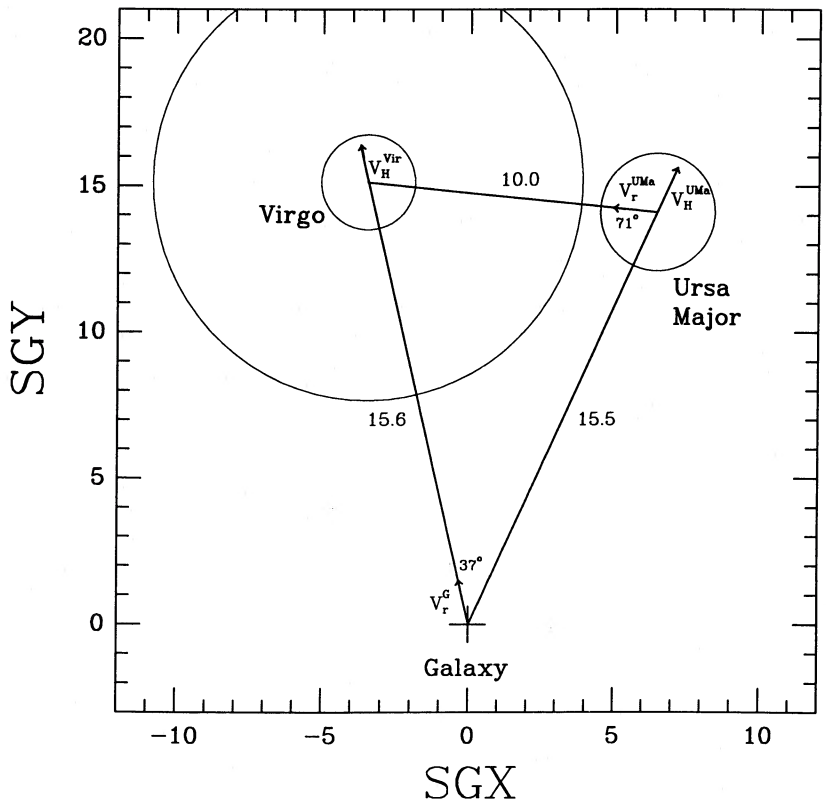

FIG. 10.—Relative geometry of the Galaxy and the Virgo and Ursa Major Clusters. The three entities all lie close to the supergalactic plane. Circles that correspond to the 6° radius of the Virgo Cluster and the 7°.5 radius of the Ursa Major Cluster are shown. A larger circle is drawn around the Virgo Cluster with a radius that corresponds to 28°. Galaxies within this circle are expected to be falling toward Virgo. The Galaxy and the Ursa Major Cluster are retarded from Hubble expansion by velocity components directed toward Virgo of V_r^G and V_r^{UMa}.

The value of H_0 we derive here agrees very favorably with that derived by Aaronson *et al.* (1986) using the infrared TF relation to derive distances to 10 clusters in the range 4000–11,000 km s^{-1}. They determine $H_0 = 92$ km s^{-1} Mpc^{-1} which, with our zero point calibration (we have a larger distance to M31), transforms to $H_0 = 88$ km s^{-1} Mpc^{-1}. What follows is a description of the status of the various sources of uncertainty in our determination of H_0 and the prospects for future improvement.

i) *Well-determined Quantities*

The small dispersion of the TF relations would indicate that with proper corrections to extinction and line widths the TF relations are capable of providing distances of high precision. As a result, very precise ($\sim 5\%$) *relative* distances for the Ursa Major and Virgo Clusters have been established. The *relative* distance modulus to a cluster with N observed members can be determined with an uncertainty of $\sim 0.3/N^{1/2}$, which is inconsequential compared to the other errors if $N \geq 20$.

There is some ambiguity in the composition of the Virgo sample because of the possibility of contamination from an infalling population, but the associated uncertainty is only $\sim 5\%$.

ii) *Principle Accountable Uncertainties*

The two primary accountable sources of error in our determination of H_0 are the error associated with the small number of local calibrators and the uncertainty vis-a-vis our model of the local velocity field. The error associated with the local calibration is $\sim 0.25/N^{1/2}$ mag where $N = 3$, or 7% in distance. There are roughly 15 well-resolved systems that ultimately could be used as calibrators, so the present uncertainty in this area could be cut in half.

We attribute 9% uncertainty to our limited understanding of the local velocity field. To reduce this uncertainty, one approach is to apply the TF relations to field galaxies to map the velocity field of the Local Supercluster. We are currently analyzing data for ~ 100 field galaxies in a preliminary attempt to do just this. Another approach would be to apply the local calibration directly to distant samples in the domain where Hubble expansion dominates peculiar motions (e.g., Bothun *et al.* 1987).

iii) *Uncertainties Outside the Error Budget*

To be quite clear, the error estimate *includes* the dispersion/$N^{1/2}$ uncertainty in the fit of the observed relationships to the local calibrators but *excludes* uncertainties in the distances of these calibrators. However, these uncertainties are expected to be comparable to our adopted errors. Feast and Walker (1987) estimate the uncertainty in the Cepheid zero point to be ~ 0.15 mag. The errors associated with the relative distance between the LMC and the three calibrating galaxies is probably ~ 0.2 mag (see references given in Table 4). Also, the error estimate does not take into account conceivable differences between the calibrator and cluster galaxies, although a preliminary analysis of a sample of ~ 80 field galaxies indicates that any differences are small (Pierce 1988). While we think the constraints on Virgocentric retardation and local peculiar motions are within our estimated uncertainties, it is all too possible that there will be surprises in the velocity field that make a mockery of our

error estimates. There is some comfort that such surprises will not be too severe, though, due to the reasonable agreement between our result (85 km s^{-1} Mpc^{-1}) and the value of 88 km s^{-1} Mpc^{-1} (with our zero point) found by Aaronson *et al.* (1986) from the analysis of clusters up to 8 times further away.

VI. SUMMARY

We have shown that with accurate CCD photometry in conjunction with photometrically derived inclinations the dispersion in the TF relations for the *R*, and *I* bands is only ~ 0.25 mag (1 σ) or 12% in distance. The dispersion in the *B* band is greater (~ 0.35 mag), presumably due to variations in the global stellar population of galaxies at a given mass. We find no detectable difference in the slope of the TF relations between the high and relatively low density regions of the Local Supercluster as represented by the Virgo Cluster and the Ursa Major Cluster. We find only a slight indication of a morphological-type dependence of the TF relations. This evidence suggests that the TF relations can be safely applied in both cluster and field environments, although severe stripping of H I should still be a concern for very dense clusters. We find that the use of aperture magnitudes (e.g., *H* band photometry) results in artificially high slopes to the TF relations and that with global magnitudes the slope reaches a maximum value of ~ 8.0 near the *I* band wavelength. This result would indicate that $L \propto V_{\max}^{3.2}$.

It is plausible that foreground and background galaxies are projected upon the core of the Virgo Cluster. The velocities of the majority of the systems with deviant distance estimates are consistent with a model that has these galaxies infalling into the cluster for the first time.

We obtained a distance scale calibration based on photometry of M31, M33, and NGC 2403 and derive distances to the Ursa Major and Virgo clusters of 15.5 ± 1.2 and 15.6 ± 1.5 Mpc, respectively. Assuming a Virgocentric deceleration of 300 km s^{-1} at the Galaxy, we derived a value for the Hubble constant of 85 ± 10 km s^{-1} Mpc^{-1}. The dominant sources of error are the preliminary nature of the velocity field model and $N^{1/2}$ statistics with only three calibrators. The error estimate does not include uncertainties in the distances of the local calibrators, nor conceivable differences between the calibrator and cluster galaxies, nor does it include the possibility that there are significant velocity components that have not been modeled.

We take this opportunity to recall the major contributions to the topics discussed here by Marc Aaronson. Thanks go to Robert Hlivak, who developed the IFA CCDs, to Mike Cawson for the GASP software, and to Jim Heasley for the "1 inch telescope" used to obtain images of M31 and M33. M. J. P. wishes to extend special thanks to his wife Pamela for her continued support over the years. M. J. P. also wishes to acknowledge the support of the Honolulu chapter of the ARCS foundation for support during 1986 and 1987. This research has been supported NSF grant AST 86-15974. CCD research at the Institute for Astronomy is partially supported by NSF grant AST 86-15631.

REFERENCES

Aaronson, M. 1986, in *Galaxy Distances and Deviations from Universal Expansion*, ed. B. Madore and R. B. Tully (Dordrecht: Reidel), p. 55.
Aaronson, M. Bothun, G., Mould, J. R., Huchra, J. P., Schommer, R. A., and Cornell, M. E. 1986, *Ap. J.*, **302**, 536.
Aaronson, M., Huchra, J. P., and Mould, J. R. 1979, *Ap. J.*, **229**, 1.
Aaronson, M., Huchra, J. P., Mould, J. R., Schechter, P. L., and Tully, R. B. 1982*a*, *Ap. J.*, **258**, 64.
Aaronson, M., *et al.* 1982*b*, *Ap. J. Suppl.*, **50**, 241.
Aaronson, M., and Mould, J. R. 1983, *Ap. J.*, **265**, 1.
Appleton, P. N., and Davies, R. D. 1982, *M.N.R.A.S.*, **201**, 1073.
Binggeli, B., Tammann, G. A., and Sandage, A. 1987, *A.J.* **94**, 251.
Bothun, G. D., Aaronson, M., M. Schommer, R. A., Huchra, J. P., and Mould, J. R. 1984, *Ap. J.*, **278**, 475.
Bothun, G., and Mould, J. R. 1987, *Ap. J.*, **313**, 629.
Bottinelli, L., Gouguenheim, L., Paturel, G., and de Vaucouleurs, G. 1980, *Ap. J. (Letters)*, **242**, L153.
———. 1983 *Astr. Ap.*, **118**, 4.
———. 1984 *Ap. J.*, **280**, 34.
Bottinelli, L., Gouguenheim, L., Paturel, G., and Teerikorpi, P. 1986, *Astr. Ap.*, **156**, 157.
Burstein, D., and Heiles, C. 1978, *Ap. J.*, **225**, 40.
Burstein, D., Rubin, V. C., Thonnard, N., and Ford, W. K., Jr. 1982, *Ap. J.*, **253**, 70.
Christian, C. A., and Schommer, R. A. 1987, *A.J.*, **93**, 557.
Cousins, A. W. J. 1976, *Mem. R.A.S.*, **81**, 25.
Davis, L. E., Cawson, M., Davies, R. L., and Illingworth, G. 1985, *A.J.*, **90**, 169.
de Vaucouleurs, G. 1961, *Ap. J. Suppl.*, **6**, 213.
———. 1981, in *10th Texas Symposium on Relativistic Astrophysics, Ann. NY Acad. Sci.*, ed. R. Ramaty and F. C. Jones (New York: New York Academy of Science), p. 90.
———. 1982, *Ap. J.*, **253**, 520.
de Vaucouleurs, G., Peters, W. L., and Corwin, H. G., Jr. 1977, *Ap. J.*, **211**, 319.
Dressler, A. 1984, *Ap. J.*, **281**, 512.
Dressler, A., Faber, S. M., Burstein, D., Davies, R. L., Lynden-Bell, D., Terlevich, R. J., and Wegner, G. 1987, *Ap. J. (Letters)*, **313**, L37.
Feast, M. W., and Walker, A. R. 1987, *Ann. Rev. Astr. Ap.*, **25**, 345.
Fernie, J. D. 1983, *Pub. A.S.P.*, **95**, 782.
Fisher, J. R., and Tully, R. B. 1981, *Ap. J. Suppl.* **47**, 139.
Freedman, W. L. 1985, in *Cepheids: Theory and Observations*, ed. B. Madore (Cambridge: Cambridge University), p. 225.
———. 1987, private communication.
Ftaclas, C., Fanelli, M. N., and Struble, M. F. 1984, *Ap. J.*, **282**, 19.
Giovanelli, R., and Haynes, M. P. 1983, *A.J.*, **88**, 881.
Giraud, E. 1986, *Astr. Ap.*, **174**, 23.
———. 1987, *Astr. Ap.*, **180**, 57.
Guhathakurta, P., van Gorkom, J. H., Kotanyi, C. G., and Balkowski, C. 1987, preprint.
Harris, W. E., Fitzgerald, M. P., and Reed, B. C. 1981, *Pub. A.S.P.*, **93**, 507.
Haynes, M. P., and Giovanelli, R. 1986, *Ap. J.*, **306**, 466.
Helou, G., Giovanardi, C., Salpeter, E. E., and Krumm, N. 1981, *Ap. J. Suppl.*, **46**, 267.
Helou, G., Hoffman, G. L., and Salpeter, E. E. 1984, *Ap. J. Suppl.*, **55**, 433.
Hlivak, R. J., Henry, J. P., and Pilcher, C. B. 1984, *Proc. Soc. Photo-Opt. Instr. Eng.*, **445**, 112.
Hlivak, R. J., Pilcher, C. B., Howell, R. R., Colucci, A. J., and Henry, J. P. 1982, *Proc. Soc. Photo-Opt. Instr. Eng.*, **331**, 96.
Hoffman, G. L. 1987, private communication.
Hoffman, G. L., Helou, G., Salpeter, E. E., Glossen, J., and Sandage, A. 1987, *Ap. J. Suppl.*, **63**, 247.
Holmberg, E. 1958, *Medd. Lunds Astr. Obs.*, Ser. II, No. 136.
Huchra, J. P. 1984, in *The Virgo Cluster of Galaxies*, ed. O. G. Richter and B. Binggeli (Garching: European Southern Observatory), p. 181.
Huchra, J. P., Davis, M., Latham, D., and Tonry, J. 1983, *Ap. J. Suppl.*, **52**, 89.
Johnson, H. L. 1968, in *Nebulae and Interstellar Matter*, ed. B. Middlehurst and L. Aller (Chicago: University of Chicago Press), p. 167.
Kraan-Korteweg, R. C. 1984, in *The Virgo Cluster of Galaxies*, ed. O. G. Richter and B. Binggeli (Garching: European Southern Observatory), p. 409.
Landolt, A. 1983, *A.J.* **88**, 439.
Lilje, P. B., Yahil, A., and Jones, B. J. T. 1986, *Ap. J.*, **307**, 91.
Madore, B. F. 1985, in *Cepheids: Theory and Observation*, ed. B. Madore (Cambridge: Cambridge University), p. 166.
Madore, B. F., McAlary, C. W., McLaren, R. A., Welch, D. L., Neugebauer, G., and Mathews, K. 1985, *Ap. J.*, **294**, 560.
Pierce, M. J. 1988, Ph.D thesis, University of Hawaii.
Pritchet, C. J., and van den Bergh, S. 1987, *Ap. J.*, **316**, 517.
Richter, O. G., and Huchtmeier, W. K. 1984, *Astr. Ap.*, **132**, 253.
Richter, O. G., Tammann, G. A., and Huchtmeier, W. K. 1987, *Astr. Ap.*, **171**, 33.
Roberts, M. S. 1978, *A.J.*, **83**, 1026.
Rubin, V. C., Burstein, D., Ford, W. K., Jr., and Thonnard, N. 1985, *Ap. J.*, **289**, 81.
Sandage, A. 1987, in *IAU Symposium 124, Observational Cosmology*, ed. A. Hewitt, G. Burbidge, and L. Fang (Dordrecht: Reidel), p. 1.
———. 1988, preprint.
Sandage, A., and Tammann, G. A. 1982, *Ap. J.*, **256**, 339.
———. 1984, *Nature*, **307**, 326.
Schechter, P. L. 1980, *A.J.*, **85**, 801.

Schwarz, U. J. 1985, *Astr. Ap.*, **142**, 273.
Tammann, G. A., and Sandage, A. 1968, *Ap. J.*, **151**, 825.
———. 1985, *Ap. J.*, **294**, 81.
Teerikorpi, P. 1987, *Astr. Ap.*, **173**, 39.
Tully, R. B. 1987, *Nearby Galaxies Catalog* (Cambridge: Cambridge University).
Tully, R. B., and Fisher, R. 1977, *Astr. Ap.*, **54**, 661.
Tully, R. B., and Fouqué, P. 1985, *Ap. J. Suppl.*, **58**, 67.
Tully, R. B., Mould, J. R., and Aaronson, M. 1982, *Ap. J.*, **257**, 527.
Tully, R. B., and Shaya, E. J. 1984, *Ap. J.*, **281**, 31.
Visvanathan, N. 1981*a*, *J. Ap. Astr.*, **2**, 67.
Visvanathan, N. 1981*b*, *Astr. Ap.*, **100**, L20.
———. 1983, *Ap. J.*, **275**, 430.
Warmels, R. H. 1986, Ph.D. thesis, University of Groningen.
Welch, D. L., McAlary, C. W., McLaren, R. A., and Madore, B. F. 1986, *Ap. J.*, **305**, 583.
Welch, D. L., McLaren, R. A., Madore, B. F., and McAlary, C. W. 1987, *Ap. J.*, **321**, 162.
Yahil, A., Tammann, G. A., and Sandage, A. 1977, *Ap. J.*, **217**, 903.
Zwicky, F., Herzog, E., and Wild, P. 1961–1963, *Catalogue of Galaxies and of Clusters of Galaxies*, Vols. **1** and **2** (Pasadena: California Institute of Technology).

M. J. PIERCE and R. B. TULLY: Institute for Astronomy, 2680 Woodlawn Drive, Honolulu, HI 96822